Spectroscopic and photorefractive characterization of cadmium telluride crystals codoped with vanadium and manganese

Robert N. Schwartz
Hughes Research Laboratories, 3011 Malibu Canyon Road, Malibu, California 90265

Chen-Chia Wang
NEC Research Institute, 4 Independence Way, Princeton, New Jersey 08540

Sudhir Trivedi and Gomatam V. Jagannathan
Brimrose Corporation of America, 7720 Belair Road, Baltimore, Maryland 21236

Frederic M. Davidson
Department of Electrical and Computer Engineering, Johns Hopkins University, Baltimore, Maryland 21218

Philip R. Boyd and Unchul Lee
Army Research Laboratory, Fort Belvoir, Virginia 22060
(Received 9 January 1997)

Electron paramagnetic resonance spectroscopy, secondary-ion mass spectrometry, and moving space charge field techniques were used to characterize semi-insulating cadmium telluride crystals codoped with vanadium and manganese. Photorefractive two-wave-mixing gains were observed for CdTe:Mn,V that were a factor of ~ 2 larger than that measured for singly doped CdTe:V. Secondary-ion mass spectrometry and electron paramagnetic resonance spectroscopy were used to establish the chemical identities, concentration levels, and charge states of the dopants that govern the photorefractive response in this semiconductor material. In CdTe:V,Mn only the Mn^{2+} EPR was observed; this result, combined with the photorefractive data, provides information regarding the existence of a manganese-related ionization level in the band gap of CdTe. [S0163-1829(97)03323-7]

Photorefractive materials have applications in many areas[1] including image processing, holographic storage,[2] and optical beam combining.[1] The space charge electric fields formed inside photorefractive materials modulate the refractive index of the host materials via the electro-optic effect, which in turn causes the diffraction of incident optical fields and therefore provides the foundation for photorefractive applications. In general, semiconductor photorefractive materials have the advantages of significantly faster response times and better sensitivity in both the visible and near-infrared wavelength regions compared to conventional oxide-based materials. In particular, cadmium telluride crystals doped with vanadium were found to have the best sensitivity among the known semiconductor photorefractive materials.[3] We report in this paper the observation of significant photorefractive two-wave-mixing gains in the diffusion-field limit in cadmium telluride samples codoped with both vanadium and manganese (CdTe:V,Mn). Moving space charge field effects[4] were used to characterize the samples and revealed photorefractive properties in good agreement with those obtained from conventional photorefractive two-wave-mixing experiments. In addition, secondary-ion mass spectrometry (SIMS) and electron paramagnetic resonance (EPR) spectroscopy were used to probe the chemical identities, concentration levels, and charge states of the dopants that govern the photorefractive response in this semiconductor material. A detailed description of the procedures and results are presented below.

The vanadium and manganese codoped CdTe crystals were grown by the vertical Bridgman technique. The starting concentrations of vanadium and manganese in the melt were equal to 5×10^{19} cm^{-3}. Stoichiometric amounts of high-purity cadmium and tellurium along with the dopants were vacuum sealed in the graphitized fused silica ampoule. The total amount of starting materials in the ampoule was 100 g. They were reacted and melted in a three-zone furnace for 48 h. After allowing the melt to homogenize for 24 h, the crystals were grown by translating the ampoule at a rate 1.5 mm/h. The temperature gradient in the solidification region was 7–8 °C/cm. After the growth was complete, the ampoule was cooled to room temperature over 24 h.

Secondary-ion mass spectrometry was used to determine the dopant levels of V and Mn incorporated in the CdTe host. SIMS measurements were accomplished using an Atomika 3000-30 (Ionprobe A-DIDA).[5,6] The positive-ion mass spectra were obtained with an oxygen cold cathode source operated at 9 keV, and with a primary ion beam current of 900 nA. Mass spectra were obtained for the manganese- and vanadium-doped CdTe samples as well as for the manganese and vanadium precursors. A survey scan on the doped CdTe sample was run from mass 10 to mass 220. After analyzing these data and identifying most of the peaks above mass 80 as Cd and Te isotopes and their respective oxides, we collected all subsequent SIMS data only between 10 and 80 amu. In addition to the expected peaks for the major constituents, peaks were identified at mass numbers 50, 51, and 55 for the vanadium isotopes and manganese, respectively. Oxide peaks for these species were also detected at 66, 67, and 71 amu. The SIMS data qualitatively

confirmed the presence of vanadium and manganese in roughly equal concentration in the CdTe sample; full quantification was not possible because of a lack of appropriate standards. In the SIMS mass spectra for the doped CdTe sample we also observed a substantial peak at mass 27. After eliminating primary ion beam contamination as a source of mass 27, this peak was assigned to an aluminum impurity. In addition to aluminum at mass 27, other impurities detected during the SIMS analysis of the CdTe:Mn,V sample included magnesium at mass numbers 24, 25, and 26, sodium at mass 23, and calcium at mass 40; the count rates for these impurities were significantly lower than those of manganese and vanadium.

It was demonstrated previously that dc photocurrents can be generated from semi-insulating photoconductive semiconductors by optical interference patterns traveling with constant speeds.[4] This constant speed optical fringe system causes the movement of the internal space charge electric field, which along with the coparticipation of the electrons and holes in the photoconduction process within the host material, generates the flow of photocurrent density given by[7]

$$j_\Sigma(\omega)=\frac{|m_0|^2E_D}{2\epsilon_0\epsilon_r}\frac{\omega\tau_g^2}{1+(\omega\tau_g)^2}\left\{\left(\frac{\sigma_n s_e I_0/(s_eI_0+\beta_e)}{1+\mu_e\tau_e k_BTK_g^2/e}\right)^2-\left(\frac{\sigma_p s_h I_0/(s_hI_0+\beta_h)}{1+\mu_h\tau_h k_BTK_g^2/e}\right)^2\right\}. \quad (1)$$

Here $\omega=\omega_{\rm LO}-\omega_s$ is the relative optical frequency difference between the two interfering optical fields, $\epsilon_0\epsilon_r$ is the permittivity of the host material, $K_g=2k_0\sin\theta$ is the grating wave number, $k_0=2\pi/\lambda$ is the optical wave number in free space, and $E_D=K_gk_BT/e$ is the diffusion field. Furthermore in Eq. (1), the electron (hole) mobility-lifetime product is denoted as $\mu_e\tau_e(\mu_h\tau_h)$, optical excitation cross sections as $s_{e,h}$, thermal generation rates as $\beta_{e,h}$, and $|m_0|$, the modulation index, is given by $|m_0|=2(P_sP_{\rm LO})^{1/2}/(P_s+P_{\rm LO})$, where $P_{\rm LO}$ (P_s) is the local oscillator (signal) laser power density and $I_0=P_{\rm LO}+P_s$. The electron (hole) conductivity is given by $\sigma_n=e\mu_en_0$ $(\sigma_p=e\mu_hp_0)$, where n_0 (p_0) is the electron (hole) concentration. The space charge field formation time is denoted as τ_g and given by

$$\tau_g^{-1}=\left[1+\frac{\epsilon_0\epsilon_rk_BTK_g^2}{e^2}\frac{N_D}{N_A(N_D-N_A)}\right]\times\left\{\frac{\sigma_n/\epsilon_0\epsilon_r}{1+\mu_e\tau_ek_BTK_g^2/e}+\frac{\sigma_p/\epsilon_0\epsilon_r}{1+\mu_h\tau_hk_BTK_g^2/e}\right\}. \quad (2)$$

It is clear from Eqs. (1) and (2) that the mobility-lifetime products of free charge carriers, as well as the hole-to-electron conductivity ratio μ_hp_0/μ_en_0, can be determined by measuring the photocurrent density at various grating spacings. In addition, the effective trap concentration $N_{\rm eff}=N_A(N_D-N_A)/N_D$, where N_D is the concentration of the deep-level donors and N_A that of the trapping sites, can be deduced from the grating spacing dependence of τ_g, as given by Eq. (2). The experimental setup used to determine the photocurrent versus grating spacing characteristic curves of the CdTe:V,Mn sample is shown in Fig. 1. The heterodyne phase-locked loop was used to frequency offset the two independent lasers that operated at the wavelength of

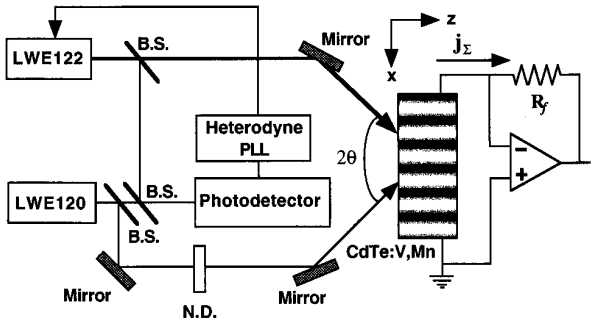

FIG. 1. Experimental setup. B.S. denotes beam splitter, N.D. denotes neutral density filter, PLL denotes phase-locked loop.

$\lambda=1.064$ μm at an adjustable value. The two optical wave fronts interfered inside the CdTe:V,Mn crystal of dimensions 4 mm×5 mm×5 mm and an interelectrode spacing of 5 mm. The conductivity of the sample increased from $\sigma_n+\sigma_p=7.5\times10^{-11}$ $(\Omega\ {\rm cm})^{-1}$ in the dark to 1.9×10^{-7} $(\Omega\ {\rm cm})^{-1}$ under the typical illumination conditions used in these experiments, which indicated that the thermal generation rates are negligible compared to photoexcitation rates of free charge carriers for this particular sample. Figure 2 shows the measured photocurrent versus grating spacing at various relative optical frequency offset values. Curve fitting using the Nelder-Meade algorithm[8] revealed that the sample was predominantly *n*-type with negligible hole concentrations. The mobility-lifetime product for electrons was found to be $\mu_e\tau_e=1.64\times10^{-5}$ cm^2/V, which agrees well with previous results.[3] The grating spacing dependence of the grating formation time was also measured and is illustrated in Fig. 3 in which the solid line is a theoretical curve based on Eq. (2) and the effective trap concentration was determined to be $N_{\rm eff}=1.15\times10^{14}$ cm^{-3}. This value for $N_{\rm eff}$ is not unreasonable because (i) even though the starting concentrations for manganese and vanadium in the melt are $\sim5\times10^{19}$ cm^{-3}, the segregation coefficient for these transition metals in CdTe is $\sim(1-2)\times10^{-3}$ and (ii) the ratio of filled-to-unfilled traps is typically on the order of 10^{-2}. Thus, roughly 1 out of

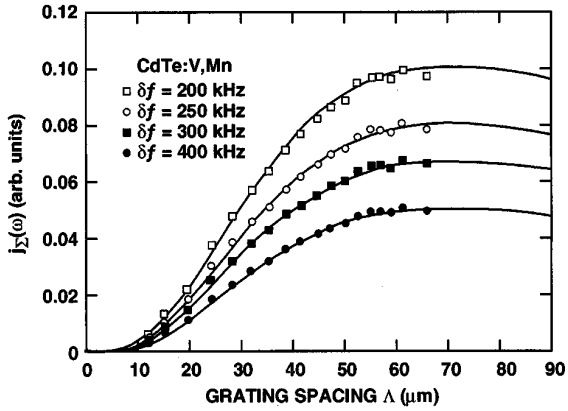

FIG. 2. Measured photocurrent outputs vs grating spacings at various laser carrier frequency offsets. The solid lines are fitting curves based on the material parameters: $\mu_e\tau_e=1.64\times10^{-5}$ cm^2/V and $\mu_hp_0/\mu_en_0=2.2\times10^{-7}$ signifying the absence of holes in this particular CdTe:Mn,V sample. The optical power levels were $P_{\rm LO}=47.38$ mW/cm^2 and $P_S=0.58$ mW/cm^2.

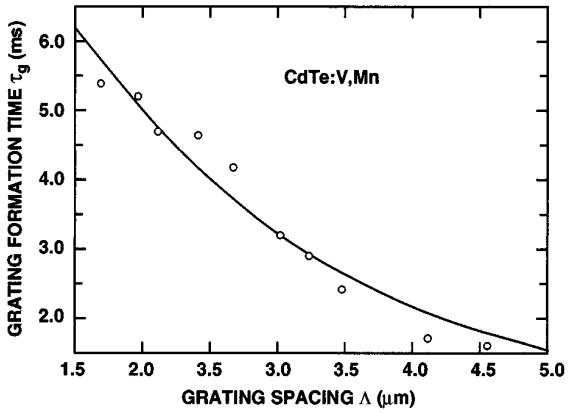

FIG. 3. Grating formation times vs the grating spacings. The solid curve is a theoretical curve based on the material characteristics $\mu_e\tau_e = 1.64\times10^{-5}$ cm^2/V and $\mu_h p_0/\mu_e n_0 = 2.2\times10^{-7}$. The optical power levels were $P_{\rm LO} = 23.05$ mW/cm^2 and $P_S = 0.16$ mW/cm^2.

100–1000 dopant ions incorporated in the crystal are available to generate or trap photocarriers.

As a consistency check, we also measured the photorefractive two-wave-mixing gain at various grating spacings in the absence of any externally applied electric fields. The results are shown in Fig. 4 and, with the values of $\mu_e\tau_e$ and $\mu_h p_0/\mu_e n_0$ determined earlier, the effective trap concentration was found to be $N_{\rm eff} = 2.96\times10^{14}$ cm^{-3}, in good agreement with the value obtained from the moving space charge field measurements. A comparison between the CdTe:V,Mn crystal investigated in this paper and a photorefractive CdTe:V crystal studied earlier[7] revealed that, under similar experimental conditions, the photorefractive two-wave-mixing gain of the doubly doped CdTe:V,Mn sample was almost *twice* that of the singly doped CdTe:V sample, even though its optical absorption coefficient was only 45% that of the CdTe:V crystal. This enhancement of photorefractive two-wave-mixing gain can be attributed to the absence of electron-hole competition effects in the CdTe:V,Mn crystal, which is consistent with the EPR results described below.

Electron paramagnetic resonance spectroscopy was used to determine the charge states of manganese and vanadium in

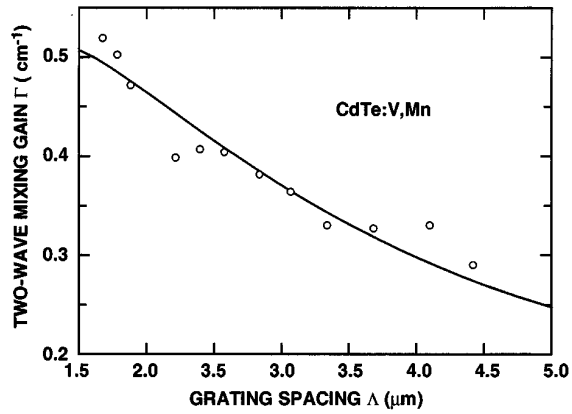

FIG. 4. Degenerate two-wave-mixing gain vs the grating spacing. The incident optical power levels were $P_{\rm LO} = 91.9$ mW/cm^2 and $P_S = 2.4$ mW/cm^2.

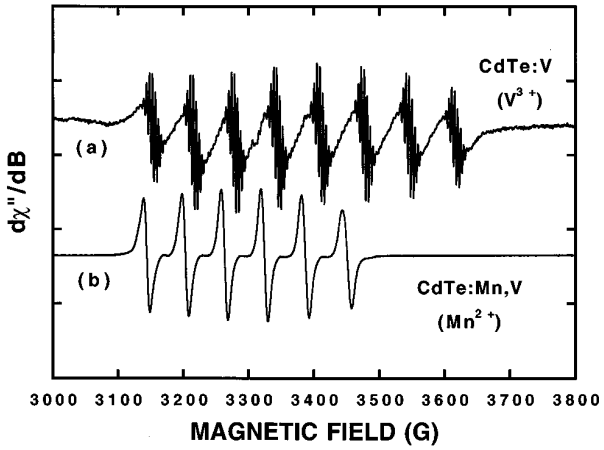

FIG. 5. *X*-band EPR spectra: (a) CdTe:V recorded at 5 K with the magnetic field $\mathbf{B}_0$ parallel to the [001] direction, $\nu = 9.26036$ GHz; and (b) CdTe:Mn,V recorded at 4.4 K with the magnetic field $\mathbf{B}_0$ parallel to the [111] direction, $\nu = 9.26146$ GHz.

CdTe:Mn,V. The EPR measurements were performed using a Varian E-109 homodyne *X*-band spectrometer equipped with a Bruker model B-H15 digital magnetic-field controller. For measurements at low temperatures, an Oxford Instruments ESR-9 continuous-flow helium cryostat system was used. Our previous work, as well as that of others, on singly doped CdTe:V has shown that vanadium exists in two different charge states $V^{3+}(3d^2, {}^3A_2)$ (Refs. 9 and 10) and $V^{2+}(3d^3, {}^4T_1)$ (Ref. 11), thus forming a donorlike defect state in CdTe. Shown in Fig. 5(a) is the EPR spectrum of CdTe:V recorded at 5 K with the magnetic field $\mathbf{B}_0$ parallel to the [001] direction. The octet of lines, which is the vanadium signature corresponding to the electron-nuclear hyperfine interaction involving the ^{51}V ($I = 7/2$, 99.75% natural abundance) nuclide, has been assigned to V^{3+}.[9–11] Superimposed on each ^{51}V hyperfine component is additional structure. This well-resolved structure is produced by hyperfine interaction with nearby Cd nuclei [^{111}Cd (12.75%) and ^{113}Cd (12.26%); both $I = 1/2$].[9,10]

In contrast, the EPR of the doubly doped CdTe:Mn,V is quite different, as shown in Fig. 5(b). This spectrum is the characteristic six-line spectrum of Mn^{2+} (^{55}Mn, $I = 5/2$, 100% natural abundance), with $g = 2.00597$ and ^{55}Mn hyperfine constant $\mathcal{A}_{\rm Mn} = 0.0057$ cm^{-1} which agree well with previously reported values.[12] The lines are quite broad, most likely due to the high concentration of paramagnetic ions, and hence no resolved hyperfine structure with the Cd nuclei was observed. It is also important to note that in CdTe:Mn,V *no EPR spectral feature that could be assigned to either V^{3+} or V^{2+} were observed.* This observation is very important since, given that the concentration of Mn and V are comparable in CdTe:Mn,V, one infers that the Fermi level (E_f) is located above the (V^{2+}/V^{3+}) ionization level. This is illustrated in Fig. 6, which shows the positions of E_f and the (Mn^{1+}/M^{2+}) and (V^{2+}/V^{3+}) ionization levels in the band gap of CdTe. Here the location E_f is only approximate; whereas for the vanadium-related level experimental results place it at $E(V^{2+}/V^{3+}) = E_{\rm VB} + 0.94$ eV,[11] and a recent calculation locates a manganese-related level at $E(Mn^{1+}/Mn^{2+}) = E_{\rm VB} + 1.4$ eV.[13] This latter result is interesting since there is some controversy regarding the exis-

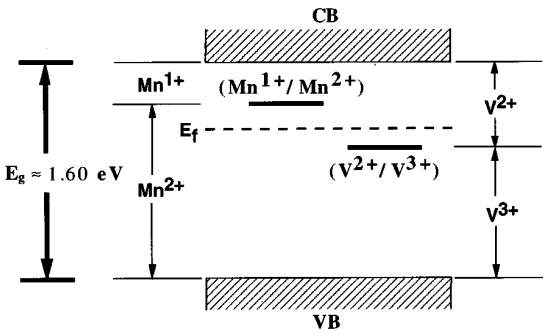

FIG. 6. Schematic energy-level diagram depicting the positions of the ionization levels for vanadium and manganese codoped in CdTe. The broken line indicates the approximate position of the Fermi level E_f as deduced from the EPR data.

tence of an ionization level in the band gap of CdTe associated with Mn.[14–16] As indicated above, our photorefractive measurements on doubly doped CdTe:Mn,V show an enhanced photorefractive two-wave mixing gain over that measured in singly doped CdTe:V. This enhancement may be explained if an additional *donor* ionization level in the vicinity of the (V^{2+}/V^{3+}) level is postulated. In particular, if this level lies closer to the conduction-band edge, the efficiency of electron photoionization relative to that of hole photoionization would be enhanced. This, in turn, would lead to a reduction in the electron-hole competition factor and, hence, to an increase in the photorefractive two-wave mixing gain. Thus, these photorefractive results, along with the fact that only the Mn^{2+} EPR is observed in codoped CdTe:Mn,V, provide supporting evidence for the existence of a (Mn^{1+}/Mn^{2+}) ionization level in the band gap of CdTe. It should also be pointed out that, because of the location of E_f, the dominant species present in the codoped material will be Mn^{2+} and V^{2+}. The optical properties of these ions, especially for Mn^{2+},[17] are different from that of V^{3+},[18,19] which is the dominant species in singly doped CdTe:V when the Fermi level lies below the (V^{2+}/V^{3+}) ionization level. Therefore, the differences in the intrinsic optical properties of the various ions may account for the reduction in the optical absorption observed in CdTe:Mn,V relative to CdTe:V. As a final note, evidence has been provided from recent photoluminescence measurements for the $V^{1+}(3d^4, {}^5T_2)$ charge state in high-resistivity CdTe:V.[20] This implies the existence of a second vanadium-related ionization level, i.e., (V^{1+}/V^{2+}). It is anticipated, however, that this charge-transfer level will be an *acceptor* level, consistent with the observation of a similar vanadium-related level in ZnTe:V.[21]

In conclusion, we have demonstrated that significant photorefractive two-wave-mixing gain can be achieved by doping cadmium telluride crystals with both vanadium and manganese. Moving space charge field techniques were used to characterize the photorefractive properties of the sample. These yielded results that agreed well with those from conventional photorefractive two-wave-mixing experiments and previous studies. SIMS and EPR spectroscopy were also used to characterize the codoped material. The EPR results, in conjunction with the photorefractive data, offer supporting evidence for the presence of a manganese-related ionization level in the band gap of CdTe.

This work was supported by BMDO through SBIR Phase II, Contract No. DASG60-93-C-0066 to Brimrose Corporation and was monitored by U.S. Army Strategic Defense Command, Huntsville, Alabama. It is a pleasure to thank Dr. Barry A. Wechsler of Hughes Research Laboratories for stimulating discussions on various aspects of this work.

[1] *Photorefractive Materials and their Applications I and II*, edited by P. Günter and J.-P. Huignard, Topics in Applied Physics Vols. 61 and 62 (Springer-Verlag, Berlin, 1989); P. Yeh, *Introduction to Photorefractive Nonlinear Optics* (Wiley, New York, 1993).

[2] M. Jeganathan and L. Hesselink, J. Opt. Soc. Am. B **11**, 1791 (1994).

[3] A. Partovi, J. Millerd, E. Garmire, M. Ziari, W. Steier, S. Trivedi, and M. Klein, Appl. Phys. Lett. **57**, 846 (1990).

[4] Chen-Chia Wang and F. Davidson, Opt. Lett. **20**, 1035 (1995).

[5] A. Bennignhoven, F. G. Rudenauer, H. W. Werner, *Secondary Ion Mass Spectrometry: Chemical Analysis* (Wiley, 1987, New York), Vol. 86.

[6] R. G. Wilson, F. A. Stevie, and C. W. Magee, *Secondary Ion Mass Spectrometry* (Wiley, New York, 1989).

[7] F. Davidson, C. C. Wang, and S. Trivedi, Opt. Commun. **111**, 470 (1994).

[8] A. Wouk, in *New Computing Environments: Microcomputers in Large-Scale Computing*, edited by A. Wouk (Society for Industrial and Applied Mathematics, Philadelphia, 1987).

[9] H. J. von Bardeleben, J. C. Launay, and V. Mazoyer, Appl. Phys. Lett. **68**, 1140 (1993).

[10] R. N. Schwartz, M. Ziari, and S. Trivedi, Phys. Rev. B **49**, 5274 (1994).

[11] P. Christmann, B. K. Meyer, J. Kreissl, R. Schwarz, and K. W. Benz, Phys. Rev. B **53**, 3634 (1996).

[12] J. Lambe and C. Kikuchi, Phys. Rev. **119**, 1256 (1960).

[13] M. Illgner and H. Overhof, Semicond. Sci. Technol. **11**, 977 (1996).

[14] A. Zunger, in *Solid State Physics: Advances in Research and Applications*, edited by H. Ehrenreich and D. Turnbull (Academic, Orlando, 1986), Vol. 39, p. 275.

[15] J. Kreissl and H.-J. Schulz, J. Cryst. Growth **161**, 239 (1996).

[16] E. Rzepka, Y. Marfaing, M. Cuniot, and R. Triboulet, Mat. Sci. Eng. D **16**, 262 (1993).

[17] A. B. P. Lever, *Inorganic Electronic Spectroscopy*, 2nd ed. (Elsevier, Amsterdam, 1984).

[18] B. Briat, F. Ramaz, A. Hamri, H. J. von Bardeleben, J. C. Launay, and V. Mazoyer, Semicond. Sci. Technol. **10**, 1629 (1995).

[19] P. Peka, M. U. Lehr, H.-J. Schulz, R. Schwarz, and K. W. Benz, Appl. Phys. A **58**, 447 (1994).

[20] P. Peka, H. R. Selber, H.-J. Schulz, R. Schwarz, and K. W. Benz, Solid State Commun. **98**, 677 (1996).

[21] P. Peka, M. U. Lehr, H.-J. Schulz, U. W. Pohl, J. Kreissl, and K. Irmscher, Phys. Rev. B **53**, 1907 (1996).